Wireless Power Transfer, 2017, 4(2), 113–119. © Cambridge University Press, 2017
doi:10.1017/wpt.2017.8

WIRELESSLY POWERING: THE FUTURE

Sidelobe reduction with a GaN active array antenna

NAOKI HASEGAWA AND NAOKI SHINOHARA

This work proposes a tunable sidelobe reduction method based on a GaN active-antenna technique, in which the output radio frequency power is controlled by the DC drain voltage of the amplifiers. In this study, a 1 × 4 array of active antenna with GaN amplifiers is designed and fabricated. GaN amplifiers capable of up to 10 W-class power output are fabricated and arranged for a four-way active-array antenna. The fabricated single-stage GaN amplifier offers a maximum power-added efficiency of 59.6% and a maximum output power of 39.3 dBm. The maximum output power is decreased to 36.5 dBm upon decreasing the operating drain voltage from 55 to 35 V. In this study, a 4.5 dB sidelobe reduction is demonstrated in a 1 × 4 active antenna based on this output power difference for each amplifier.

Keywords: Microwave power transfer (MPT), GaN amplifier, Sidelobe reduction, Active array antenna

Received 30 April 2017; Revised 24 August 2017; Accepted 24 August 2017

I. INTRODUCTION

Microwave power transfer (MPT) technology has been investigated since the 1960s. Recently, many MPT systems have been proposed, such as ultra-long-range wireless power transfer for space solar-power satellite and wireless power supplies for sensor networks, electric vehicles, and mobile phones [1–3]. Most of these studies have been based on a microwave beam forming by array-antenna techniques. The recent advances in MPT are closely tied with these of antenna and radio frequency (RF) power semiconductor technologies.

The RF GaN amplifier serves an important role in MPT transmission system. The GaN semiconductor offers a wider band gap than those mode of Si or GaAs, and faster electron mobility than those mode of SiC. Hence, GaN semiconductor techniques are necessary to meet the demands of next-generation high-power RF systems. Recently, high-power and high-efficiency GaN amplifiers have been developed [4–16]. For instance, Kuroda *et al.* reported a high-efficiency *C*-band (5.8 GHz) GaN amplifier with 71.4% power-added efficiency (PAE) in 2010 [17]. In addition, Kobayashi *et al.* reported a high-power *S*-band (2.1 GHz) GaN solid-state power amplifier with kW-class power output in 2013 [18]. The transmitted power and efficiency are directly affected by the operating power and the DC–RF conversion efficiency of the GaN amplifier. Therefore, these novel GaN amplifiers are extremely useful for high-power and high-efficiency MPT systems.

Recently developed long-range MPT systems conventionally use array-antenna techniques for controlling the microwave beam. In the MPT system, the beam control techniques are critically necessary to improve the transmission efficiency and to reduce the level of the sidelobes. In 2015, Ishikawa and Shinohara reported the formation of a flat-topped beam by implementing phase tuning for each antenna, and this was used in an MPT system installed on a vehicle roof [2].

Sidelobe-reduction techniques have also been studied in the context of passive antenna design in conventional studies. In general, the operated RF power is larger than the microwave power required for communication. MPT systems must not interfere with traditional wireless communication or affect the immediate environment. Hence, it is desirable to reduce the level of the sidelobes derived from the array antenna. Low-sidelobe antenna techniques with element phase control have been reported [19–24]. In addition, sidelobe reduction by amplitude control has been investigated [25, 26]. For instance, Chen *et al.* proposed a low-sidelobe array antenna with a filtering microstrip antenna in 2017 [27]. In these conventional designs, the sidelobe is mainly reduced using non-uniform division techniques.

It is difficult to tunable control the sidelobe level via the conventional circuit approach. However, situationally tunable sidelobe control is required for MPT systems developed for EVs, mobile phones, and wireless sensors. In long-range MPT systems, active-array antennas are generally used. In this study, the active-array antenna configuration consisting of antenna elements with GaN power amplifiers, as shown in Fig. 1(a), is assumed. In conventional studies, sidelobe reduction by an effectual amplitude distribution on the surface of antenna was reported by Taylor in 1955 [28]. In this work, sidelobe reduction was achieved using GaN active-antenna techniques. The input–output characteristics of an amplifier are shown in Fig. 1(b). In general, it is possible to control the saturated power output of the amplifier by adjusting the operating drain DC power level. In this work,

Research Institute for Sustainable Humanosphere, Kyoto University, Gokasho, Uji, Kyoto 611-0011, Japan. Phone: +81 774 38 3853
Corresponding author:
N. Hasegawa
Email: naoki_hasegawa@rish.kyoto-u.ac.jp

https://doi.org/10.1017/wpt.2017.8 Published online by Cambridge University Press

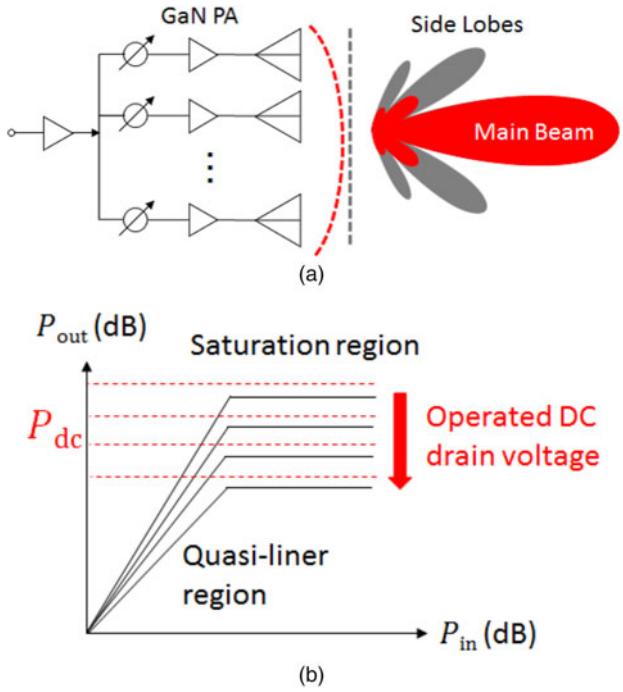


Fig. 1. Low-sidelobe active-array antenna: (a) active array antenna configuration and (b) amplifier input–output characteristics for various operating DC drain voltages.

the saturated output power of GaN amplifiers is controlled to realize sidelobe reduction. The advantage of this sidelobe reduction method based on an active-antenna approach is that it is possible to tune the sidelobes by adjusting the operating DC power of the amplifier.

In this study, a tunable sidelobe reduction technique with a GaN active-array antenna is proposed. First, a single-stage GaN amplifier is designed and fabricated. Second, a four-way GaN active-array antenna is designed and fabricated. Then, the resulting low-sidelobe active antenna is characterized.

II. AMPLIFIER DESIGN AND FABRICATION

In this study, a power GaN HEMT (Sumitomo Elec, SG0601C) is used for the amplifier design. The load- and source-side input impedances of the chip are determined via a load-pull simulation with a non-linear model using Kesignt ADS, as shown in Table 1. In Table 1, Z_{L1} and Z_{L2} are the load-side input impedances at the 5.8 GHz fundamental frequency and the 11.6 GHz second harmonic frequency, respectively. Z_S is the source-side input impedance at the fundamental frequency. In this simulation, the input RF power, P_{in}, the gate DC voltage, V_g, and the drain DC voltage, V_d, are 30 dBm, −2.5, and 50 V, respectively. Under these impedance conditions, a 67.1% PAE and a 41.2 dBm RF output power (P_{out}) are calculated by the simulation. Hence, in the following amplifier design, these conditions are targeted for the amplifier circuits.

Table 1. Calculated load-pull impedances at the fundamental and second harmonic frequencies with 30 dBm RF input.

	Impedances (Ω)	PAE (%)	P_{out} (dBm)
Z_{L1}	$25.6 + j53.3$		
Z_{L2}	$0 + j36.7$	67.1	41.2
Z_S	$2.9 + j11.6$		

A) Single-stage amplifier

First, the single-stage GaN amplifier is designed and fabricated. The designed GaN amplifier consists of matching networks, bias lines, and a harmonic treatment circuit as shown in Fig. 2(a). The DC cut capacitors are mounted in the matching network and the bypass capacitors are mounted in the bias lines. The harmonic circuit, which is designed with short stabs, as shown in Fig. 2(a), treats a second harmonic. These circuits are fabricated on a dielectric substrate of Arlon AD1000 (with $\varepsilon_r = 10.2$, $\tan\delta = 0.0023$, and thickness of 0.8 mm). The load- and source-side input impedances of the designed circuit are $Z_{L1} = 28.2 + j53.6$ Ω, $Z_{L2} = 5.8 + j35.4$ Ω, and $Z_S = 6.5 + j10.1$ Ω. The single-stage GaN amplifier is fabricated as shown in Fig. 2(b). The GaN HEMT chip is mounted on a copper plate, which is connected to the circuits by wires. The circuit substrates are also mounted on the copper plate.

The measured input–output characteristics are shown in Fig. 3. In Figs 3(a) and 3(b), the effects of the drain voltage levels on the output power, P_{out}, and on the PAE are illustrated. According to Fig. 3(a), the maximum output power is 39.3 dBm when $V_d = 40$ V, which decreases to 36.5 dBm when the drain voltage level is reduced to $V_d = 35$ V. In contrast, the maximum PAE peaks at 59.6% when $V_d = 40$ V,

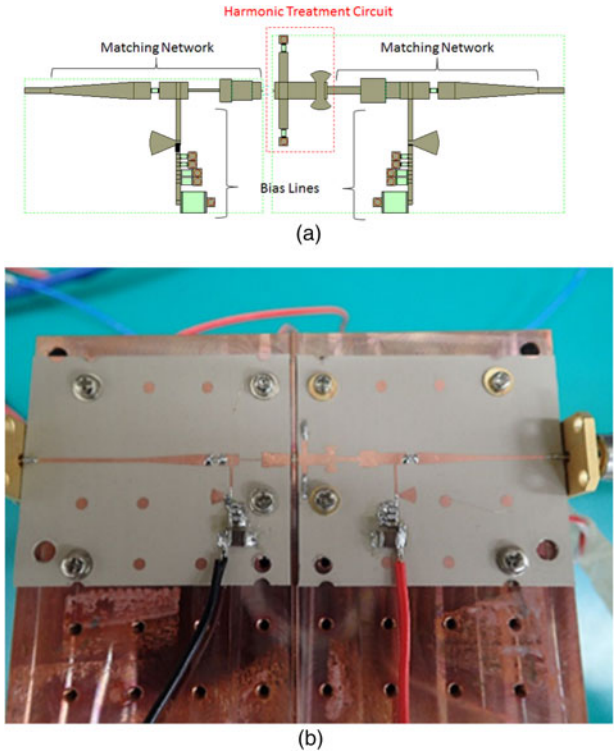


Fig. 2. (a) Designed GaN amplifier layout and (b) image of the fabricated amplifier.

https://doi.org/10.1017/wpt.2017.8 Published online by Cambridge University Press

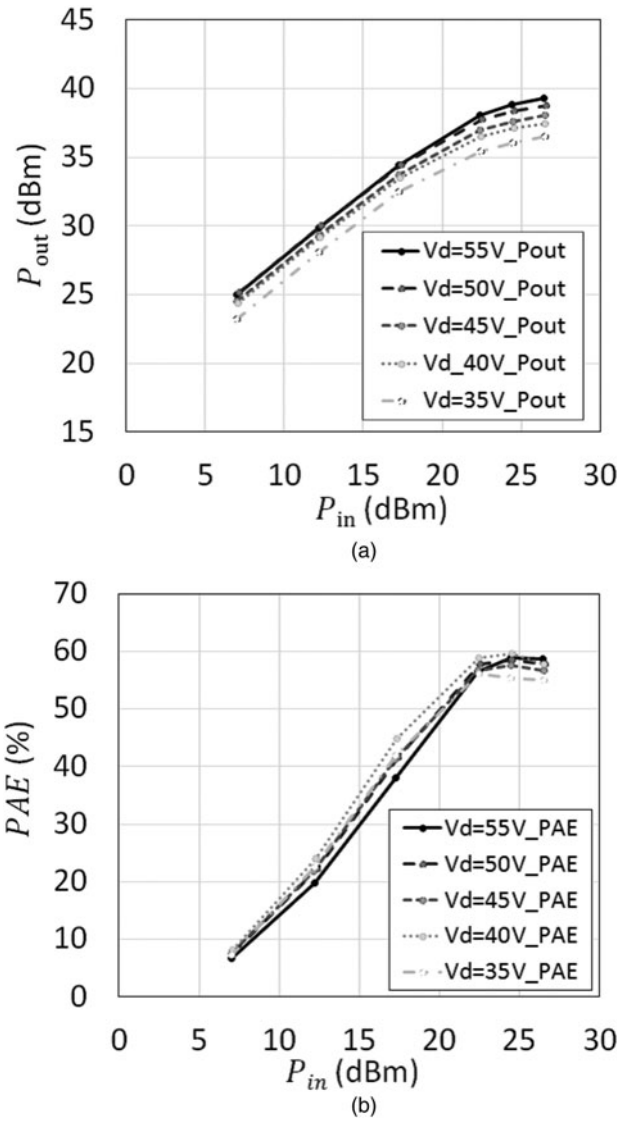


Fig. 3. Measured input–output characteristics at operating the DC drain voltage between 35 and 55 V: (a) measured output power P_{out} and (b) measured PAE.

$P_{in} = 24.5$ dBm. In each drain voltage condition tested, maximum PAEs over 50% are confirmed. According to the results, the amplifier output power can be controlled between 36.5 and 39.3 dBm with minimal reduction in the PAE, which facilitates sidelobe reduction in the GaN active-array antenna.

B) Four-way amplifier

In this study, the sidelobe reduction is based on a four-way GaN active-array antenna. Hence, a four-way amplifier is designed and fabricated, as shown in Fig. 4. The fabricated amplifier circuits are mounted to a copper plate and packed in an aluminum case of 90 mm width, 162 mm length, and 58 mm height.

The measured maximum PAE and P_{out} under difference applied drain voltages are illustrated in Fig. 5. In these measurements, the maximum input power is 25.36 dBm. The measured maximum output power increases as the drain

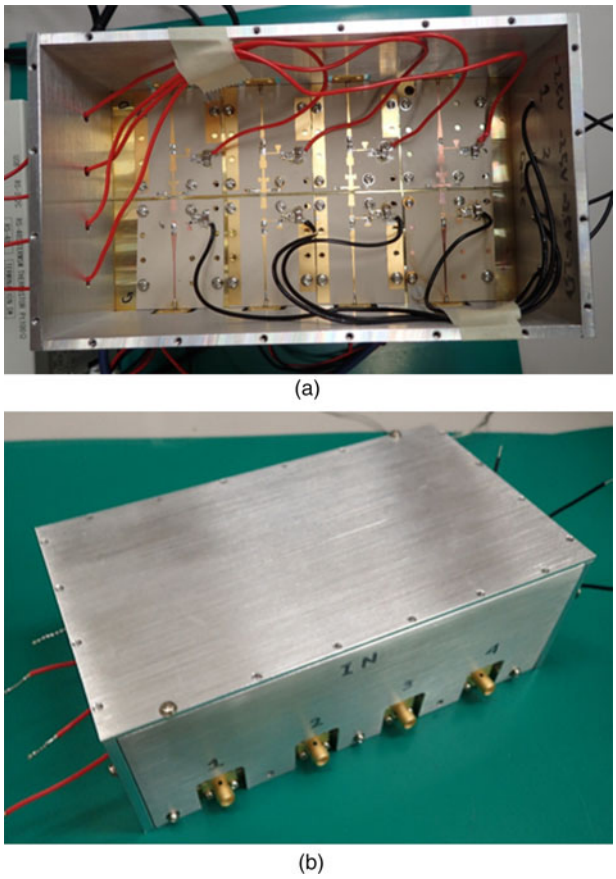


Fig. 4. Fabricated four-way GaN amplifier.

voltage increases. On the other hand, the measured PAE decreases with increasing drain voltage, reaching a minimum of 50.1% when the drain voltage is 55 V. However, the PAE remains within a range of 50–60% for all drain voltages tested.

The factors affecting the input–output characteristics, such as the maximum PAE and output power, are measured. However, the output phase of the amplifier may be shifted for each drain voltage. Therefore, the GaN amplifier is measured using a system comprising of a vector network analyzer, a driver amplifier, and other RF components as shown in Fig. 6. Using this system, the *S*-parameters of the amplifier, including the isolators, the 40 dB driver amplifier, the directional coupler, and the 30 dB attenuator, are measured. The amplitude and phase compositions of the *S*-parameters include the independent characteristics of these components. However, the effect of the drain voltage on the fabricated GaN amplifier, which hardly depends on the component characteristics, is also considered using this measurement system.

III. LOW-SIDELOBE ANTENNA DESIGN

The 1 × 4 array antenna with a circular patch antenna, shown in Fig. 7(a), is designed and fabricated. A high-frequency three-dimensional EM field simulator (CST Microwave Office) is used in this design. This antenna is fabricated on a dielectric Nippon Piller Packing NPC-F260A ($\varepsilon_r = 2.55$, $\tan\delta = 0.0018$, and thickness of 1.6 mm) substrate. The

https://doi.org/10.1017/wpt.2017.8 Published online by Cambridge University Press

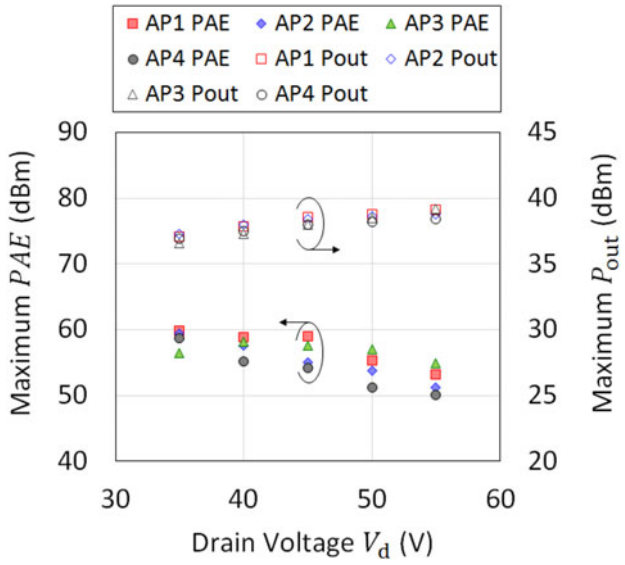


Fig. 5. Measured maximum PAE and P_{out} as a function of the drain voltage.

diameter of the patch antenna is 17.4 mm and the feed pin is shifted 2.7 mm from the center. The calculated and measured values of the reflection coefficient $|S_{11}|s$ are illustrated in Fig. 7(b). Both theoretical and experimental results show that $|S_{11}|$ is reduced to <-10 dB at 5.8 GHz.

The antenna radiation patterns were calculated based on the measured amplifier output power and phase; the results are illustrated in Fig. 8. In the calculation, the port phase and amplitude of the edge of the array antenna are fixed to the values associated with a 35 V drain voltage for the amplifier based on the measured correlation shown in Fig. 9. On the other hand, the center antennas are tuned between teh amplitude and phase associated with the 35 and 55 V drain voltage. According to Fig. 8, the second sidelobe level of 6.6 dB is reduced by tuning the port amplitude and phase conditions. The main beam amplitude is hardly reduced. The first null point and sidelobe vanish when the 55 V conditions are applied to the center antennas because of the phase difference of the amplifiers for each drain voltage condition. According to Fig. 8, removing the phase difference of the amplifiers causes the null point and sidelobe to unfold. Therefore, it is concluded that the removal of the null point and sidelobe vanish is caused by the phase difference of the amplifiers.

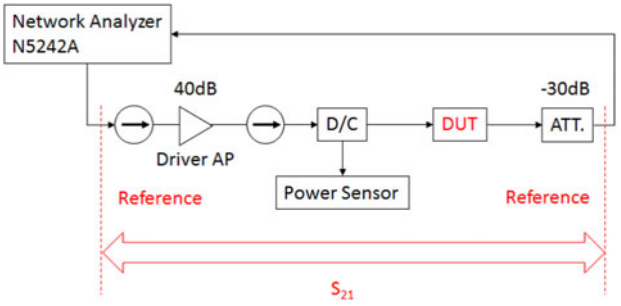


Fig. 6. Measurement system for *S*-parameters of GaN amplifier under high-power conditions using a network analyzer.

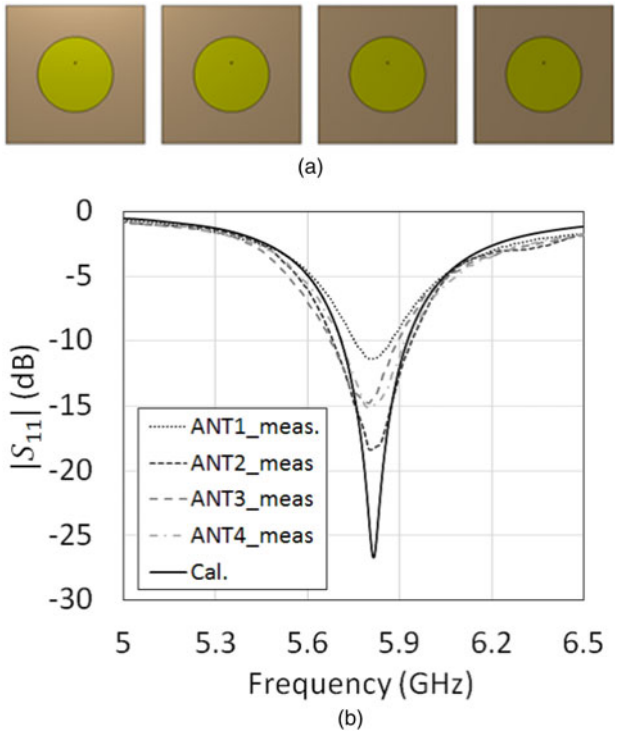


Fig. 7. Designed 1 × 4 array antenna: (a) antenna layout and (b) measured and calculated values of the antenna reflection coefficient $|S_{11}|s$.

IV. CHARACTERIZATION OF LOW-SIDELOBE ACTIVE ANTENNA

The fabricated four-way amplifier and antenna are combined, as shown in Fig. 10(a). The active-antenna component

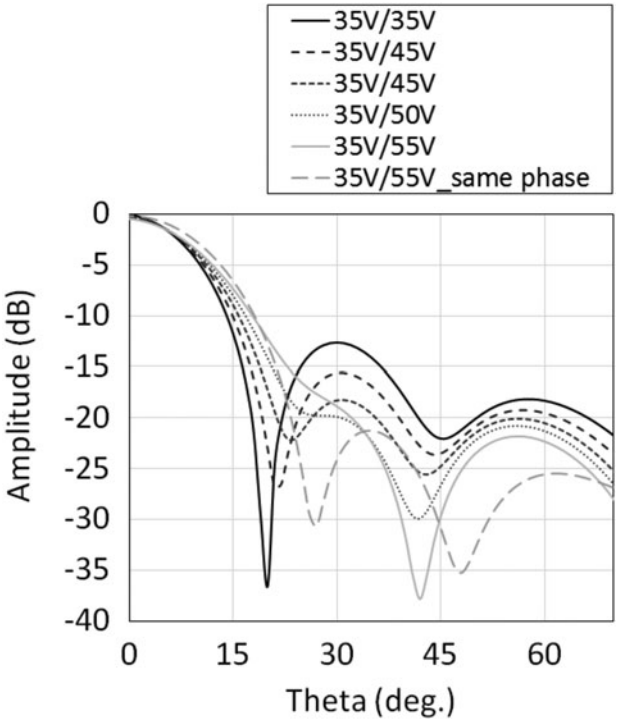


Fig. 8. Calculated antenna radiation patterns based on measured four-way amplifier output characteristics for each drain voltage condition.

https://doi.org/10.1017/wpt.2017.8 Published online by Cambridge University Press

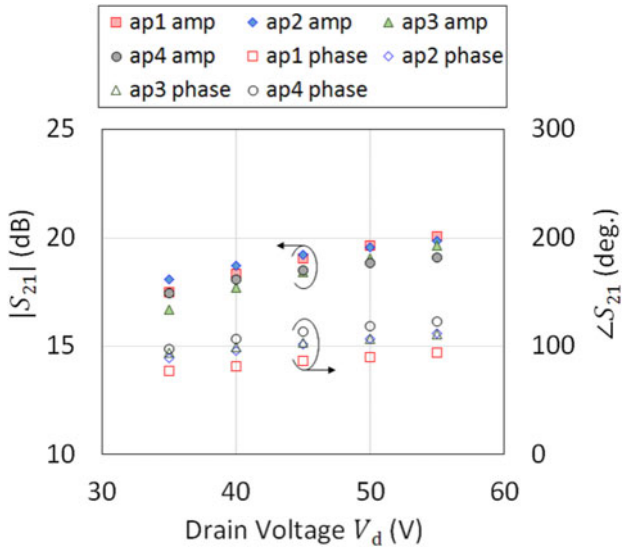


Fig. 9. Measured GaN amplifier *S*-parameters associated with different drain voltages.

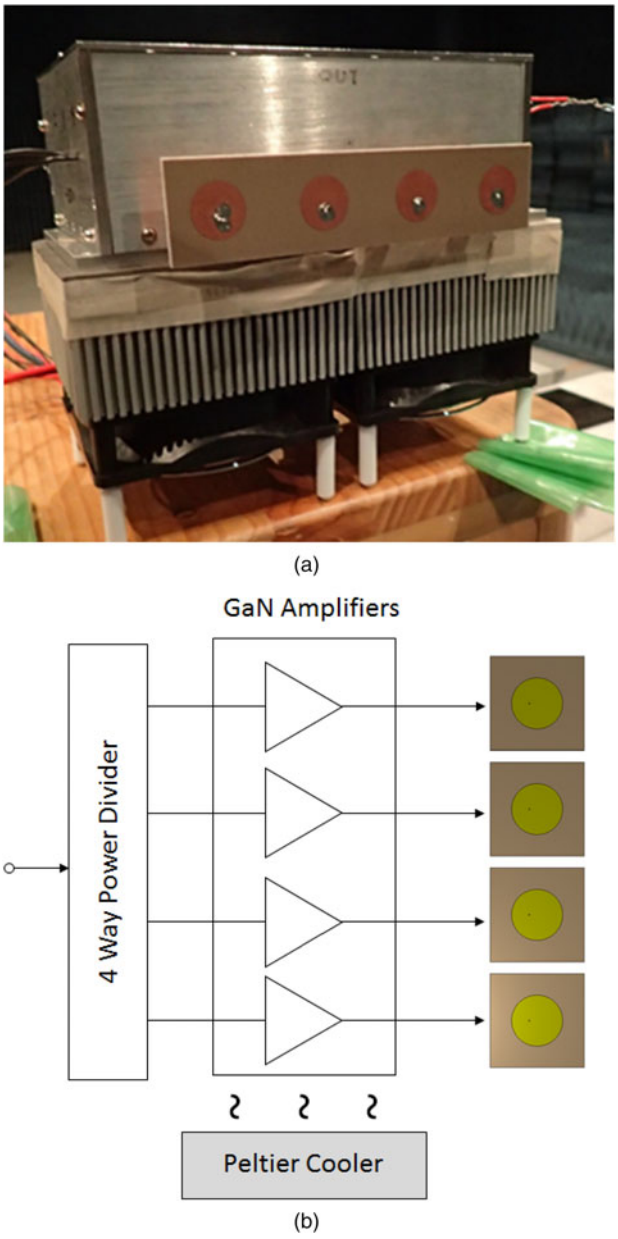


Fig. 10. Fabricated 1 × 4 GaN active array antenna: (a) image and (b) configuration of GaN active-array antenna.

consists of the GaN amplifier, the antennas, and the power divider as shown in Fig. 10(b). The GaN amplifier is placed on a Peltier cooler (VICS LVPU-70), which serves to precisely control the surface temperature; the cooler can absorb up to 70 W, which is sufficient to eliminate the thermal effects on the GaN amplifier.

The measured main beam and sidelobe levels for various drain voltage conditions are illustrated in Fig. 11. In this measurement, the drain voltage of the center amplifiers is tuned between 35 and 55 V and the edge amplifiers are fixed to 35 V. According to Fig. 11, the measured main beam levels agree with the calculated results and sidelobe levels decrease as the drain voltage of the center amplifiers increase. In addition, by tuning the center-amplifier drain voltage from 35 to 55 V, the sidelobe level of 4.52 dB is reduced. In this experiment, the ability to reduce the sidelobe level of more than 50% by tuning the amplifier drain voltage is demonstrated.

Furthermore, the equivalent isotropically radiated power (EIRP) for the front direction of the antenna is measured, which is important to characterize the performance of the active antenna. The EIRP is defined by the following equation,

$$EIRP = P_{in} \times G_{ant}, \quad (1)$$

where P_{in} is the input power to the antenna under test and G_{ant} is the isotropic gain of antenna. In this study, G_{ant} is measured by the gain-transfer method with a gain-standard dipole antenna. The measured EIRP of the GaN active antenna and dipole antenna are shown in Fig. 12. The measured maximum EIRP is 55.6 dBm at the 35/55 V drain voltage condition; this falls to 52.1 dBm in the 35/35 V condition because the total output power from the GaN amplifiers is reduced.

V. CONCLUSION

This study proposes a sidelobe reduction method based on a GaN active array antenna. In this method, the sidelobe level is tuned by adjusting the operating DC drain voltage of the amplifiers, which enables the situational switching of the radiation pattern. In this study, a single-stage GaN amplifier is designed and fabricated. The measured maximum output power is 39.3 dBm and the PAE is 59.6% at a 55 V DC drain voltage; when the drain voltage is decreased to 35 V, the output power decreases to 36.5 dBm. The amplifier output difference is proactively leveraged to realize sidelobe reduction. To do this, a four-way GaN amplifier is fabricated. The characteristics of the amplifiers are measured by a network analyzer and further used to calculate the antenna radiation pattern. The four-way GaN active-array antenna was tested, with the amplifier DC drain voltage varying from 35 to 55 V. According to the results, the 4.5 dB sidelobe level is reduced by tuning the operating center-amplifier drain voltage from 35 to 55 V, while the edge amplifiers are fixed to the 35 V condition. By this approach, it is possible to reduce

https://doi.org/10.1017/wpt.2017.8 Published online by Cambridge University Press

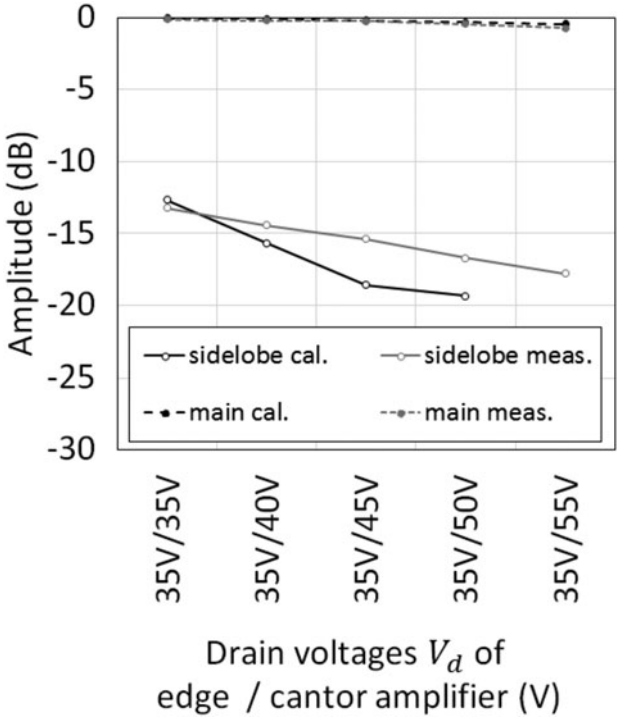


Fig. 11. Measured and calculated main beam and sidelobe amplitude for each drain voltage condition.

the sidelobe level of more than 50% by tuning the amplifier drain voltage. Finally, the maximum EIRP for the front direction is measured as 55.6 dBm when the 35 V conditions are set for the edge amplifiers and the 55 V conditions are provided for the center amplifiers; this value is reduced to 52.1 dBm upon decreasing the center amplifier DC drain voltage condition to 35 V.

In this study, tunable sidelobe reduction based on the GaN active-antenna technique has been demonstrated effectively. We expect that the proposed technique will contribute to the broad realization and implementation of MPT systems. Sidelobes can cause electromagnetic interference, affect the human body, and cause a myriad of problems. Thus, this technique is useful for the situational sidelobe reduction necessary for a variety of future long-range MPT system for EVs, mobile phones, and sensor networks.

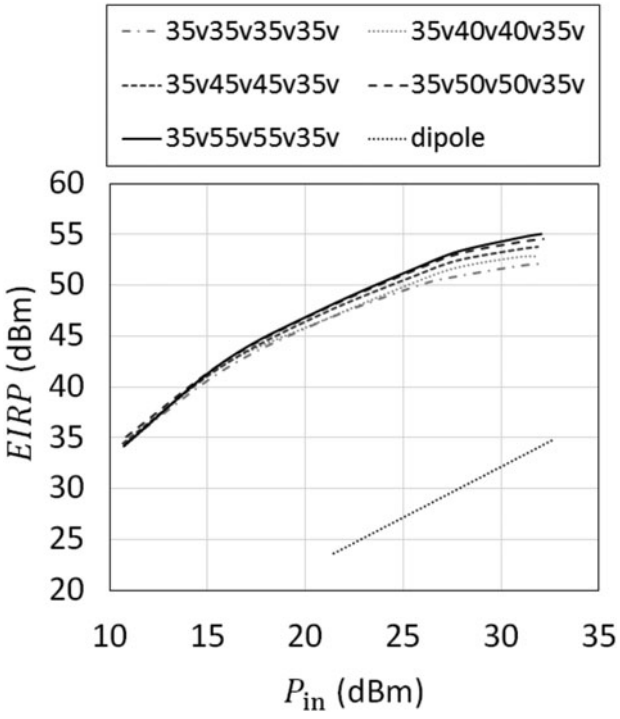


Fig. 12. Measured front-direction EIRP of GaN active array antenna.

ACKNOWLEDGEMENTS

The authors would like to thank K. Sone, T. Orihara, M. Nishihara, S. Maruyama, N. Miyazawa, T. Yamamoto, T. Imamura, N. Kuwata, and T. Fujitani from Sumitomo Electric, for providing the high-power GaN-HEMT SG0601C. The authors would also like to thank T. Mitani and members of Shinohara laboratory, Kyoto University, for helpful discussions.

REFERENCES

[1] Takano, T.: Wireless power transfer from space to earth. IEICE Trans. Electron., **E96-C** (10) (2012), 1218–1226.

[2] Ishikawa, T.; Shinohara, N.: Flat-topped forming experiment for microwave power transfer system to a vehicle roof. Wireless Power Transf., **2** (1) (2015), 15–21.

[3] Yoshida, S.; Hasegawa, N.; Kawasaki, S.: The aerospace wireless sensor network system compatible with microwave power transmission by time- and frequency-division operations. Wireless Power Transf., **2** (2) (2015), 3–14.

[4] Kanto, K.; Satomi, A.; Asahi, Y.; Kashiwabara, Y.; Matsushita, K.; Takagi, K.: An X-band 250W solid-state power amplifier using GaN power HEMTs, in Proc. IEEE Radio Wireless Symp., Orland, FL, June 2008, 77–80.

[5] Casto, M. et al. 100 W X-band GaN SSPA for medium power TWTA replacement, in Proc. IEEE Wireless Microwave Technology Conf. Clearwater Beach, FL, April 2011, 1–4.

[6] Jeong, H.C.; Yeom, K.W.: A miniaturized 2.5 GHz 8 W GaN HEMT power amplifier module using selectively anodized aluminum oxide substrate. IEICE Trans. Electron., **E95-C** (10) (2012), 1580–1588.

[7] Jeong, H.C.; Yeom, K.W.: A design of X-band 40 W pulse-driven GaN HEMT power amplifier. IEICE Trans. Electron., **E96-C** (6) (2013), 923–934.

[8] Yamashita, Y.; Nakada, T.; Kumamoto, T.; Suzuki, R.; Tanabe, M.: X-band GaN HEMT advanced power amplifier unit for compact active phased array antennas, in Proc. ICCAS-SICE, Aug. 2009, 3047–3050.

[9] Seita, H.; Kawasaki, S.: Compact and high p-power, spatial power combiner by active integrated antenna technique at 5.8 GHz. IEICE Trans. Electron., **E91-C** (11) (2008), 1757–1764.

[10] Maeda, M. et al. Source second-harmonic control for high efficiency power amplifiers. IEEE Trans. Microw. Theory Tech., **43** (12) (1995), 2952–2958.

[11] Woo, Y.Y.; Yang, Y.; Kim, B.: Analysis and experiments for high-efficiency class-F and inverse class-F power amplifier. IEEE Trans. Microw. Theory Tech., **54** (5) (2006), 1969–1974.

https://doi.org/10.1017/wpt.2017.8 Published online by Cambridge University Press

[12] Colantonio, P. et al. A C-band high-efficiency second-harmonic-tuned hybrid power amplifier in GaN technology. IEEE Trans. Microw. Theory Tech., **54** (6) (2006), 2713–2722.

[13] Grebennikov, A.: High-efficiency transmission-line GaN HEMT inverse class F power amplifier for active antenna arrays, in Proc. APMC, December 2009, 317–320.

[14] Jeong, H.C.; Oh, H.S.; Yeom, K.W.: A miniaturized WiMAX band 4-W class-F GaN @HEMT power amplifier module. IEEE Trans. Microw. Theory Tech., **59** (12) (2011), 3184–3194.

[15] Chen, K.; Peroulis, D.: Design of broadband highly efficient harmonic-tuned power amplifier using in-band continuous class-F-1/F mode transferring. IEEE Trans. Microw. Theory Tech., **60** (12) (2012), 4107–4116.

[16] Stameroff, A.N.; Ta, H.H.; Pham, A.V.; Leoni, R.E. III: Wide-bandwidth power-combining and inverse class-F GaN power amplifier at X-band. IEEE Trans. Microw. Theory Tech., **61** (3) (2013), 1291–1300.

[17] Kuroda, K.; Ishikawa, R.; Honjo, K.: Parasitic compensation design technique for a C-band GaN HEMT class-F amplifier. IEEE Trans. Microw. Theory Tech., **58** (11) (2010), 2741–2750.

[18] Kobayashi, Y.; Yoshida, Y.; Yamamoto, Z.; Kawasaki, S.: S-band GaN on Si based 1 kW-class SSPA system for space wireless applications. IEICE Trans. Electron., **E96-C** (10) (2013), 1245–1253.

[19] Goto, N.; Tsunoda, Y.: Sidelobe reduction of circular arrays with a constant excitation amplitude. IEEE Trans. Antennas Propag., **25** (6) (1977), 896–898.

[20] Will, P.M.; Keizer, N.: Low sidelobe array pattern synthesis with compensation for errors due to quantized tapering. IEEE Trans. Antennas Propag., **59** (12) (2011), 4520–4524.

[21] Juyal, P.; Shafai, L.: Sidelobe reduction of TM12 mode of circular patch via nonresonant narrow slot. IEEE Trans. Antennas Propag.., **64** (8) (2016), 3361–3369.

[22] Hodjat, F.; Hovanessian, S.: Nonuniformly spaced linear and planar array antennas for sidelobe reduction. IEEE Trans. Antennas Propag.., **26** (2) (1978), 198–204.

[23] Nasirov, S.; Levine, E.; Matzner, H.: Sidelobe reduction in uniformly-fed arrays by applying parasitic elements, in Proc ISAP 2016, 24–28 October 2016.

[24] Zainal, N.A.; Kamarudin, M.R.; Yamada, Y.; Seman, N.; Khalily, M.; Jusoh, M.: Sidelobe reduction of unequally spaced arrays for 5G applications, in Proc. 10th EuCAP, 10–15 April 2016.

[25] Huang, G.L.; Zhou, S.G.; Chio, T.H.; Hui, H.T.; Yeo, T.S.: A low profile and low sidelobe wideband slot antenna array Feb by an amplitude-tapering waveguide feed-network. IEEE Trans. Antennas Propag. **63** (1) (2015), 419–423.

[26] Nikkhah, M.R.; Mohassel, J.R.; Kishk, A.A.: Wide-band and low side-lobe array of rectangular dielectric resonator antennas with parasitic elements, in Proc. ICMCS w014, 14–16 April 2014.

[27] Chen, F.C.; Hu, H.T.; Li, R.S.; Chu, Q.Z.; Lancaster, M.J.: Design of filtering microstrip antenna array with reduced sidelobe level. IEEE Trans. Antennas Propag. **65** (2) (2017), 903–908.

[28] Taylor, T.T.: Design of line-source antennas for narrow beamwidth and low side lobes. IEEE Trans. Antennas Propag., **3** (1) (1955), 16–28.



Naoki Hasegawa was born in Aichi, Japan, on June 18, 1988. He received his B.E. degree in Electrical and Electronic Engineering from Ritsumeikan University, Siga, Japan, and his M.E. degree in Electrical Engineering from Kyoto University, Kyoto, Japan, in 2011 and 2013, respectively. He was a research associate in The Japan Aerospace Exploration Agency (JAXA) from 2013 to 2015. He is a student member of the Institute of Electronics, Information and Communication Engineers (IEICE) and the Institute of Electrical and Electronic Engineers (IEEE). His research activities include RF GaN power amplifier and antenna design for wireless power transfer and up-link satellite communications.



Naoki Shinohara received the B.E. degree in Electronic Engineering, the M.E. and Ph.D. (Eng.) degrees in Electrical Engineering from Kyoto University, Japan, in 1991, 1993, and 1996, respectively. He was a research associate in Kyoto University from 1996. From 2010, he has been a professor in Kyoto University. He has been engaged in research on Solar Power Station/Satellite and Microwave Power Transmission system. He is IEEE MTT-S Technical Committee 26 (Wireless Power Transfer and Conversion) vice chair, IEEE MTT-S Kansai Chapter TPC member, IEEE Wireless Power Transfer Conference advisory committee member, International Journal of Wireless Power Transfer (Cambridge Press) executive editor, technical committee on IEICE Wireless Power Transfer, communications society member, Japan Society of Electromagnetic Wave Energy Applications vice president, Space Solar Power Systems Society board member, Wireless Power Transfer Consortium for Practical Applications (WiPoT) chair, and Wireless Power Management Consortium (WPMc) chair.

https://doi.org/10.1017/wpt.2017.8 Published online by Cambridge University Press